Holzforschung, Vol. 60, pp. 78–84, 2006 • Copyright © by Walter de Gruyter • Berlin • New York. DOI 10.1515/HF.2006.014

Rolling shear modulus and damping factor of spruce and decayed spruce estimated by modal analysis

Sandy Isabelle Schubert[1,2,*], Daniel Gsell[2], Jürg Dual[3], Masoud Motavalli[2] and Peter Niemz[1]

[1] Institute of Building Materials, ETH Zürich, Zürich, Switzerland
[2] Structural Engineering Research Laboratory, EMPA, Duebendorf, Switzerland
[3] Institute of Mechanical Systems, ETH Zürich, Zürich, Switzerland

*Corresponding author.
Sandy Isabelle Schubert, Institute of Building Materials, ETH Zentrum CLA H31, 8092 Zürich, Switzerland
Tel.: +41-446326106
E-mail: sandy.schubert@imes.ethz.ch

Abstract

Modal analysis was used to determine the rolling shear modulus of Norway spruce samples that were either untreated or inoculated with fungi. The resonance frequencies of centimeter-range cuboids were measured using contact-less laser interferometry. A three-dimensional theoretical model describing the orthotropic behavior of the material was used to calculate the resonance frequencies. Using an iterative scheme based on the least-squares method, the value of the rolling shear modulus was then extracted. In this first investigation, the decrease in the rolling shear modulus and the weight loss of Norway spruce inoculated with white-rot fungi *Heterobasidion annosum* and *Ganoderma lipsiense* were studied for three different exposure times ranging from 4 to 12 weeks. Comparison of measured and theoretical resonance frequencies confirmed that operation was in the applicable range of the theoretical model for the inoculated specimens. A decrease in rolling shear modulus of up to 10% (*H. annosum*) and 50% (*G. lipsiense*) was found.

Keywords: *Ganoderma lipsiense*; *Heterobasidion annosum*; modal analysis; resonant ultrasound spectroscopy; rolling shear modulus; white rot.

Introduction

Fungal degradation of wood results in considerable losses in the commercial value of logs and hazards to the environment by loss of stability. Wood decay leads to decreases in weight and stiffness, as well as to changes in the damping factor and moisture content. This influences the velocity of structural wave propagation in the material and the natural frequencies of wooden structures. The aim of this work was to study the first three of these factors in an appropriate frequency and deformation range according to non-destructive testing methods using sound propagation or vibrations. These methods might be used to determine the state of degradation.

Until now, most investigators have studied the velocity of the longitudinal wave propagating along the fiber axis (v_L) (Niemz et al. 2000) or perpendicular to the growth rings (v_R) of wood (Wilcox 1988; Schwarze and Fink 1994) in specimens of centimeter size using frequencies from 300 Hz to 1 MHz. According to Bauer and Kilbertus (1991), v_R and the velocity of transverse waves propagating along either the radial or the tangential axis and polarized with respect to the other direction (along the R or T axis; v_{RT}) were significantly more sensitive to decay due to the brown-rot fungus *Gloeophyllum trabeum* than the velocities of all other principle directions. For the white-rot fungus *Coriolus versicolor*, the sensitive velocities were the velocity of the longitudinal wave propagating tangential to the growth rings, v_T, and v_{RT}.

"Ultrasonic tomography" of standing trees, as proposed by Divos and Szalai (2002) and Rust (2000), is based on time-of-flight measurements of the quasi-longitudinal wave in the radial-tangential plane on many points around the cross-section. Depending on the wavelength ($\lambda = vf^{-1}$, where f is the frequency) and the diameter of the trunk, a reasonable frequency range for measurements of this kind is 10–50 kHz. Another common approach for non-destructive testing in wood science and in many other fields is modal analysis, recently applied to standing trees by Axmon et al. (2002, 2004). Natural frequencies, which were supposed to be sensitive to *Heterobasidion annosum* decay of Norway spruce, corresponded to the "ovaling" mode and were in the range of 50 Hz to 2 kHz. The frequency of this ovaling mode depends on the diameter of the trunk, the density and the elastic constant $C_{44} = G_{RT}$ of the material, i.e., the velocity of the transversal wave $v_{RT} = \sqrt{G_{RT}\rho^{-1}}$, which was shown to be sensitive to decay in a study by Bauer and Kilbertus (1991).

Before the approach of Axmon et al. (2002, 2004) can be investigated theoretically, knowledge of the influence of fungal decay on the density and shear modulus G_{RT} is required. The shear modulus G_{RT} is by far the lowest elastic constant of softwood, and thus the lowest natural frequencies of a wooden cube depend only on G_{RT}. Hence, modal analysis of small wooden specimens was chosen in this work (see Figure 1). The frequency and deformation range of the non-destructive methods mentioned are also satisfied by this method (5–15 kHz and μm-range deformation). Experimental modal analysis identifies the natural frequencies of the specimens. In addition, the natural frequencies need to be calculated using a theoretical model. Thus, G_{RT} was determined using an iterative scheme obtained by a least-squares fit. In the literature, this method is often called resonant ultrasound spectroscopy (RUS), as reviewed by Migliori et al. (2001).

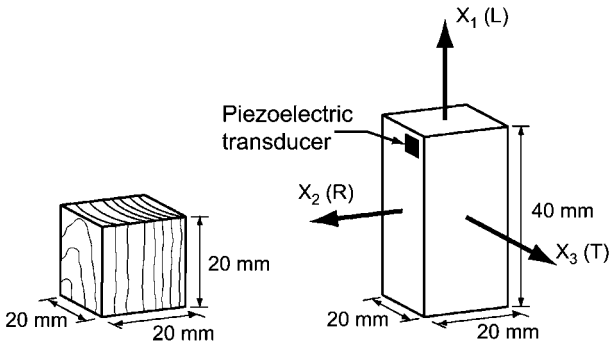

Figure 1 Definition of the coordinate system and geometry of the cube (left) and the cuboid (right). L, R and T refer to the longitudinal (fiber), radial and tangential directions, respectively.

As the material damping of wood is significantly higher than the damping of the materials used for RUS to date, modifications of the experimental set-up and the data processing were required. The shear modulus G_{RT} and the damping of untreated and inoculated Norway spruce (*Picea abies*) were determined by RUS in this investigation.

Two important white-rot fungi, *H. annosum* and *G. lipsiense* (Etheridge 1955; Worrall et al. 1983; Rayner and Boddy 1988), were chosen. According to the literature, *H. annosum* leads to preferential degradation of lignin in Norway spruce for both naturally decayed (Blanchette 1984) and laboratory decayed (Schwarze et al. 1997) wood. On the other hand, Blanchette et al. (1985) reported that *G. lipsiense* leads to selective delignification or simultaneous degradation of lignin and cellulose in birch wood under natural or laboratory decay conditions, respectively.

Materials and methods

Specimens, fungal treatment and climatic conditions

Clear wooden samples (Figure 1) were sawn from a board of spruce (*Picea abies*) tangential to the growth rings. Untreated specimens were conditioned at 20°C and 65% relative humidity (RH) before G_{RT} was determined. The number of specimens measured and their distribution over the exposure times are listed in Table 1. Subsequently the samples were dried at 103°C, weighed individually and sterilized with ethylene oxide to prevent contamination with other fungi. To establish appropriate conditions for colonization by *H. annosum* (DSM 2728, EMPA No. 620) and *G. lipsiense* (Uni Freiburg 250593.1, EMPA No. 646) all specimens were steamed twice for 10 min to achieve a moisture content of $>28\%$. The samples were inserted into Kolle flasks containing agar and covered with mycelia of either *H. annosum* or *G. lipsiense*; exposure was carried out at 22°C and 75% humidity. At the end of each exposure period, all adherent mycelia were removed and the specimens are weighed to estimate the moisture content. Before applying RUS, the decayed specimens were again conditioned at 20°C and 65% humidity. The dry weight losses and the moisture content after sample degradation were assessed by drying samples at 103°C.

Resonant ultrasound spectroscopy

Experimental set-up The experimental set-up for RUS is shown in Figure 2A. A white noise signal was generated by a function generator (Stanford Research DS345), while the bandwidth of the signal was restricted to 0–25 kHz by a low-pass filter (Krohn-Hite 3988). A piezoelectric transducer (2.80 $\times$3.85$\times$1 or 2.15$\times$2.15$\times$1 mm^3, mass $m_p<2\%$ of the specimen mass) glued to the specimen surface changes its thickness according to the amplified (Krohn-Hite 750) electrical field applied and excites the specimen. Displacement of the sample surface was determined using a heterodyne laser interferometer (Polytech OFV3001), while retro-reflective tape on the sample surface enhances the necessary reflection. A demodulator (MH PD4) was used because of the low displacement range, as explained by Dual et al. (1996). Since all expected resonance frequencies were above 1000 Hz, a high-pass filter at 500 Hz was applied to the measured signal and it was digitized by an A/D converter (NI 5911) with a sampling rate of 1 MHz and an effective vertical resolution of 17.5 bit.

Signal processing Resonance frequencies f_i and damping factors δ_j were determined by a matrix pencil algorithm as described by Hua and Sarkar (1990). The condition for applying this method is that the amplitude $y(t)$ of the signal can be described by a finite sum of M exponential functions:

$$y(t)=\sum_{j=1}^{M} A_j e^{-\delta_j t} e^{i2\pi f_j t}+n(t), \quad (1)$$

where A_j is the complex amplitude, f_i is the frequency, δ_j is the damping factor of the j-th harmonic part, $n(t)$ is the measurement noise and i is the imaginary unit. The energy content of the noise signal used is low and uniformly distributed within the frequency range considered. Hence, the structural response within the range considered has a finite number of frequencies of high energy – the resonance frequencies – and can be written in the form of Eq. (1). All steps of the signal processing procedure are described in Figure 2B.

Theoretical model The finite element method (FEM) may be used to calculate resonance frequencies, but in RUS a much faster method, based on a parametrical description of the deformation state, is necessary. As proposed by Demarest (1971), the components of the displacement were expressed using Legendre polynomials:

$$\boldsymbol{u}_i^T(\mathbf{x},t)=\mathbf{q}_i^T(t)\mathbf{P}(\mathbf{x}), \quad \text{with} \quad i=1,2,3, \quad (2)$$

where $\mathbf{q}_i$ is the time-dependent unknown coefficient vector and $\mathbf{P}$ is a matrix of polynomials describing the deformation state of the cuboid:

Table 1 Number of specimens for which the shear modulus G_{RT} was determined.

Treatment	Number of specimens tested				
	Sound	4 weeks	6 weeks	8 weeks	12 weeks
Untreated	18 (6)	–	–	–	–
G. lipsiense	14 (5)	10 (2)	10 (2)	10 (1)	–
H. annosum	15 (5)	9 (2)	–	10 (2)	10 (1)

Values in parentheses denote the number of cubic specimens.

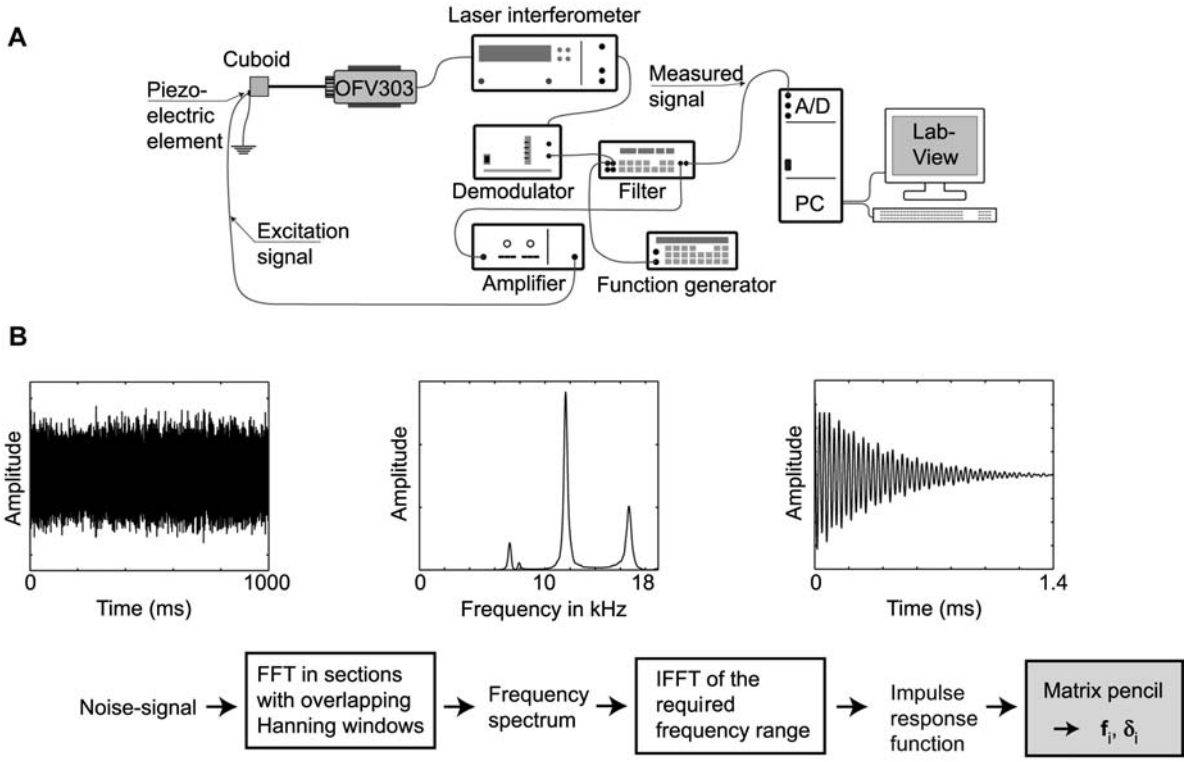

Figure 2 (A) Experimental set-up and (B) signal processing procedure.

$$\mathbf{P}(\boldsymbol{x})=[p_1,p_2,\ldots,p_N],\quad \text{with}\quad p_j=P_m\left(\frac{x_1}{b}\right)P_s\left(\frac{x_2}{c}\right)P_r\left(\frac{x_3}{d}\right), \tag{3}$$

where P is a Legendre polynomial of order m, s or r and b, c and d are the dimensions of the cuboid. For correct description of the deformation, it is necessary to satisfy the completeness of the polynomial approach, and therefore all possible permutations of the Legendre polynomial orders m, s and r for $m,s,r=0,1,\ldots,L$ subject to $m+s+r\leq L$, are selected. Hence, the size of $\mathbf{P}$ is $N=(L+3)(L+2)(L+1)$, where L is the maximum polynomial order.

Hooke's law $\boldsymbol{\sigma}(\mathbf{x},t)=\mathbf{C}\boldsymbol{\varepsilon}(\mathbf{x},t)$ is used to describe the relation between the stresses $\boldsymbol{\sigma}$ and the linear strains $\boldsymbol{\varepsilon}$ in terms of the stiffness tensor $\mathbf{C}$, where linear kinematic relations give $\boldsymbol{\varepsilon}=\mathbf{L}\mathbf{q}^T$, with $\mathbf{L}$ a matrix containing the spatial derivatives of $\mathbf{P}$. With the separational approach for the coefficients $\mathbf{q}(t)=\mathbf{a}e^{i\omega t}$ in Hamilton's principle, the following eigenvalue problem was derived:

$$(-\omega^2\mathbf{M}+\mathbf{K}(\mathbf{C}))\mathbf{a}=0, \tag{4}$$

with matrices of mass $\mathbf{M}$ and stiffness $\mathbf{K}$:

$$\mathbf{M}=\int_V \rho\mathbf{P}\mathbf{P}^T\mathrm{d}V \quad\text{and}\quad \mathbf{K}=\int_V \rho\mathbf{L}\mathbf{C}\mathbf{L}^T\mathrm{d}V. \tag{5}$$

Implementing the effect of the piezoelectric element mass m_p, the matrix $\mathbf{M}$ was extended to:

$$\boldsymbol{M}=\int_V \rho\mathbf{P}\mathbf{P}^T\mathrm{d}V+\int_{S_p}\frac{m_p}{S_p}\mathbf{P}\mathbf{P}^T\mathrm{d}S, \tag{6}$$

where S_p is the surface area onto which the piezoelectric element was glued. The accuracy of the model with the piezoelectric element was checked by comparing the results with finite element calculations using 3D solid elements. The difference between the FE calculations and the polynomial approach of polynomial order $L=15$ was approximately 0.02% and 0.6% for the first and second resonance frequency, respectively, whereas the CPU time required by the polynomial approach is less than 1/50th of that for FE calculations.

Iterative scheme Since no closed-form solution exists for the elements of the stiffness tensor $\mathbf{C}$ in Eq. (4), an iterative scheme was applied to solve the inverse problem. Reasonable starting values for the stiffness tensor $\mathbf{C}$ were chosen. As described in the Introduction, the lowest natural frequencies mainly depend on C_{44}, and thus the iteration scheme was only carried out for this elastic constant. The new values for C_{44}^n were derived from the least-squares method, minimizing the error between the measured (f_i) and calculated (f_i^{cal}) frequencies:

$$F(C_{44})=\sum_{i=1}^{M}(f_i^{\mathrm{cal}}-f_i)^2, \tag{7}$$

subject to Eq. (4). Applying the Taylor expansion around the initial value C_{44}^0, the value for the next iteration step was obtained:

$$C_{44}^n=C_{44}^0+\Delta C_{44},\quad \text{with}\quad \Delta C_{44}=F(C_{44}^0)\left(\left[\frac{\partial F(C_{44})}{\partial C_{44}}\right]_{C_{44}=C_{44}^0}\right)^{-1}. \tag{8}$$

The new value C_{44}^n is a better estimation than C_{44}^0 and is used for the subsequent step. The iteration was carried out until the changes in the values of the stiffness tensor are sufficiently small. For the results shown in the next section, the element C_{44} was determined by fitting the first two resonance frequencies; see Figure 3 for the dominant influence of C_{44}. For completeness, the values used for the stiffness tensor $\mathbf{C}$ were: $C_{11}=15600$, $C_{22}=950$, $C_{33}=650$, $C_{12}=640$, $C_{23}=350$, $C_{13}=510$, $C_{55}=750$ and $C_{66}=800$, all in MPa; the starting value for C_{44} was 35 MPa. By varying each value of the stiffness tensor $\mathbf{C}$ by

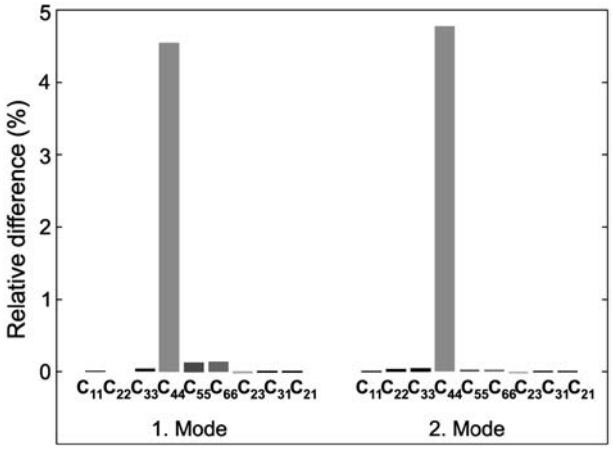

Figure 3 Relative difference in the resonance frequencies for a 10% higher value of the corresponding element of the stiffness tensor.

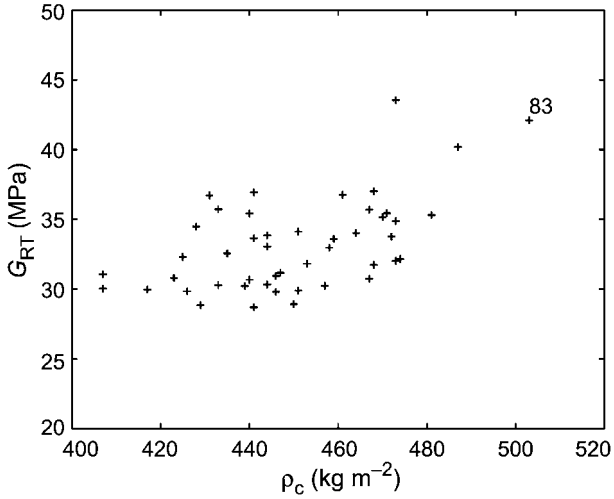

Figure 4 Shear modulus G_{RT} of 47 untreated specimens as a function of density ρ_c at 20°C and 65% RH. Mean values: $\bar{G}_{RT}=33.2\pm3$ MPa and $\bar{\rho}_c=450\pm20$ kg m^{-3}; R = 0.56.

approximately 10%, the relative differences of the extracted C_{44} varied by only 0.003–0.17%.

Results and discussion

The elastic constant $C_{44}=G_{RT}$ of the untreated wood was determined for 47 specimens, as shown in Figure 4. The mean value $\bar{G}_{RT}=33.2\pm3$ MPa, with a moisture content (MC) of 12.5 ± 0.5% is in accordance with the literature (Table 2). To compare the damping behavior of different specimens or materials, it is common to define the attenuation factor $D=\delta(2\pi f_0)^{-1}$, where f_0 is the resonance frequency. The attenuation factor D was determined for 41 specimens, with a mean value of $\bar{D}=0.016\pm0.001$.

The shear modulus G_{RT} of one control specimen was measured before and after the drying process to estimate the influence of oven drying. Before both measurements, the sample was conditioned under climate conditions of 20°C/65% RH. The estimated difference in G_{RT} was +2.3%, while the moisture content decreased from 12% to 11%.

Despite the fact that both pathogens had completely grown over the specimens after the first exposure period, *G. lipsiense* and *H. annosum* showed diverse destructive activity. The G_{RT} values for 30 specimens degraded by *G. lipsiense*, depicted in Figure 5A, are distinguishably lower value (down to 50%) than for untreated specimens. According to the lower mass loss after 4 and 8 weeks, *H. annosum* degraded the wood constituents more slowly than *G. lipsiense*. The effect on the elastic constant G_{RT} was small and could only be distinguished after 12 weeks of exposure (Figure 5B). Both pathogens resulted in slightly higher values for the attenuation factor D for inoculated compared to untreated specimens, whereas the deviation was greater for inoculated samples. The theoretical model used for calculation of the frequencies considers an orthotropic and homogeneous cuboid. Because of fungal decay, the inhomogeneity may increase and the geometry may differ slightly from a cuboid. The differences between the measured and calculated natural frequencies are a measure of the commensurability of the model. For untreated specimens, these differences for the first and second natural frequency were 0.7% on average, and a maximum error of 2%. For samples decayed by *G. lipsiense*, the mean difference (1.0%, 1.4% and 1.7%) and maximum error (1.7%, 2.5% and 5.5%) increased with exposure time (4, 6 and 8 weeks, respectively). The mean values demonstrate that the specimens were still in good agreement with the model. No significant changes could be observed for *H. annosum* based on the mean difference (0.4%, 0.6% and 0.4%) and maximum error (1.3%, 2.6% and 1.6% for 4, 8 and 12 weeks, respectively).

The weight loss, stiffness, damping and MC results for all inoculated specimens are summarized in Table 3. The equilibrium MC of the untreated and decayed specimens differed slightly, but did not result in significant changes in G_{RT}. Relative changes in the shear modulus G_{RT} were analyzed for half of the specimens by measuring their values before and after exposure under climatic conditions of 20°C/65% RH. The results of the relative measurements depicted in Figure 5C show the different relations between the decrease in stiffness and the weight loss of specimens decayed by *H. annosum* and *G. lipsiense*. Because of the potential influence of the mass of fungal mycelia on the weight loss, no linear regression analysis was carried out for the data in Figure 5. The importance of relative measurements should be emphasized. For specimen No. 83 in Figure 5, the high G_{RT} value after exposure is only due to the large stiffness

Table 2 Rolling shear modulus G_{RT} values reported in the literature.

G_{RT} (MPa)	Density (kg m^{-3})	MC (%)	Reference
35	423	9.8	Stamer (1935)
37	500	12	Hearmon (1948)
41	NS	12.5	Neuhaus (1983)
75	409	NS	Bucur and Archer (1984)
36	400	8.0–12.0	Bucur (1987)
58	447	10.0–13.0	Dumail et al. (2000)
30	450	NS	Görlacher (2002)

NS, not specified.

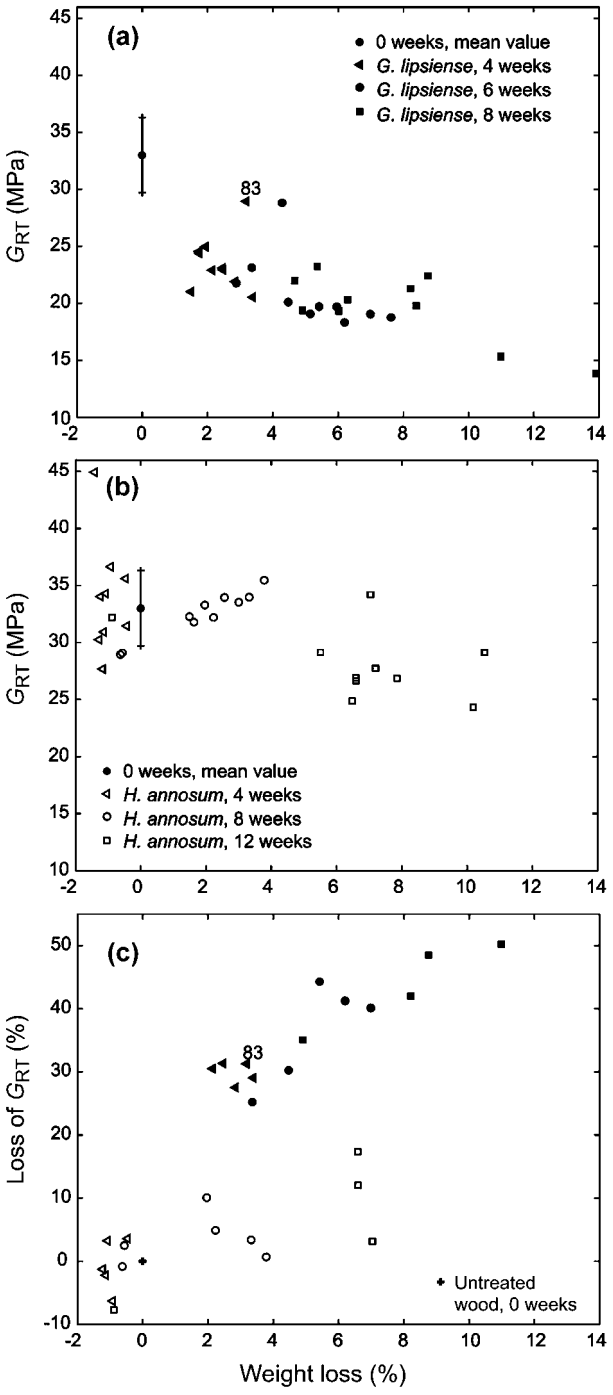

Figure 5 Rolling shear modulus G_{RT} as a function of weight loss due for (A) *G. lipsiense* and (B) *H. annosum*. (C) Relationship between the decrease in G_{RT} and weight loss.

value for the untreated specimen (Figure 4), as the percentage decrease in G_{RT} is similar to that for the other samples.

The motivation for this study was to assess the influence of fungal wood decay on elastic waves or resonances, which might be used for non-destructive testing of standing trees. Therefore, the significant information is the change in the relation between stiffness and density, i.e., the wave velocity and impedance. In our case, the variation in the velocity of the transverse wave $v_{RT} = \sqrt{G_{RT}\rho^{-1}}$ and the impedance $z_{RT} = \sqrt{\rho \cdot G_{RT}}$ describe the influence. Consequently, the velocity v_{RT} in a decayed region was related to the values for the untreated wood by the coefficient d_{vRT}:

$$d_{v_{RT}} = \frac{v_{RT}^{D}}{v_{RT}}, \quad \text{with} \quad v_{RT}^{D} = \sqrt{\frac{G_{RT}^{D}}{\rho^{D}}}, \tag{9}$$

where the superscript D indicates the values are for a decayed specimen. By analogy, the coefficient for impedance (d_{zRT}) was defined, which describes the reflection of the transverse wave. These coefficients were calculated using the results of the relative measurements in Table 4. As can be observed in Figure 6, the velocity v_{RT} and impedance z_{RT} were sensitive to the degradation pattern of *G. lipsiense*. Thus, analysis of the wave propagation and reflection phenomena or resonances represents a promising non-destructive method for detecting areas decayed by *G. lipsiense.* On the other hand, degradation by *H. annosum* in the early stages was sensitive to neither velocity nor impedance.

Until now, the change in MC because of fungal activity has been neglected in evaluation of the velocity v_{RT}. For these laboratory-decayed specimens, the higher MC would lead to an approximately 22% and 14% higher density for *H. annosum* and *G. lipsiense*, respectively, and a reduced shear modulus. Therefore, the reduction in v_{RT} due to the MC would be relevant in comparison with the decrease in stiffness after decay by *H. annosum*. Comparing this result for *H. annosum* in Norway spruce with results reported by Schwarze (1995), who measured the velocity v_R for spruce decayed by *H. annosum* and control specimens after 12 weeks of exposure, it is evident that the changes in velocity at stages with small weight loss were because of higher MC rather than a decrease in stiffness due to decay.

Conclusions

Resonant ultrasound spectroscopy was successfully applied to specimens of Norway spruce to determine the shear modulus G_{RT} and the attenuation factor D in the required frequency range. The orthotropic behavior of wood was correctly described in the three-dimensional theoretical model and the measurement was contact-less and non-destructive. Thus, the method allows evaluation of relative changes in G_{RT} due to fungal decay or different climatic conditions. The latter is also interesting for research in mechanical pulping to investigate the non-local rolling shear modulus. It should also be possible to determine the shear modulus and other elastic constants of plywood and solid wood panels, although a different geometry may be required.

Our results showed that the agreement required for the model and modeled object was met for untreated and inoculated specimens. Hence, this method can be used to study the variation of G_{RT} and damping D for various types of host-fungus relations. For *G. lipsiense*, the decrease in G_{RT} resulted in a significant change in the transverse velocity v_{RT} and the impedance z_{RT}. Whereas, degradation by *H. annosum* showed no significant influence on the relation between the decrease in stiffness and weight loss. Comparison of this result with other

Table 3 Summary of the results for *G. lipsiense* and *H. annosum*.

Exposure time	Weight loss (%)	G_{RT} (MPa)	D	Density (kg m^{-3})	MC (%)		Number of specimens
					20°/60%	After exposure	
G. lipsiense							
0 weeks	0±0	33.4±4.5	0.016±0.001	447±20	12.5±0.4	–	14
4 weeks	2.3±0.6	23.5±2.3	0.019±0.005	456±20	12.7±0.4	42.3±2.5	10
6 weeks	5.2±1.4	20.9±3.0	0.021±0.008	427±30	12.4±0.3	44.7±6.1	10
8 weeks	7.8±2.8	19.7±2.9	0.022±0.004	412±24	14.7±0.2	47.6±9.0	10
H. annosum							
0 weeks	0±0	33.3±2.7	0.016±0.002	451±16	12.7±0.5	–	15
4 weeks	−1.0±0.3	34.0±4.7	0.019±0.004	456±21	13.1±0.5	51.3±3.8	9
8 weeks	1.9±1.4	32.5±2.0	0.021±0.005	453±16	14.9±0.2	52.5±6.6	10
12 weeks	6.7±3.0	28.2±3.0	0.019±0.003	418±25	13.3±0.1	55.5±11.4	10

Table 4 Coefficients for the significant parameters as a function of the exposure time.

Exposure time	Weight loss (%)	Decrease in G_{RT} (MPa)	d_{vRT} (%)	d_{zRT} (%)	Number of specimens
G. lipsiense					
4 weeks	2.8±0.4	29.9±1.5	84.8±0.9	82.6±0.9	5
6 weeks	5.3±1.3	36.2±7.2	81.2±4.4	78.3±4.8	5
8 weeks	8.2±2.2	43.9±6.0	77.3±3.1	72.3±4.8	4
H. annosum					
4 weeks	−1.0±0.3	−0.6±3.7	99.2±1.5	101.0±2.2	5
8 weeks	1.6±1.7	3.5±3.5	98.1±1.9	98.4±2.1	5
12 weeks	4.8±3.3	6.2±9.5	98.4±3.9	95.1±6.0	4

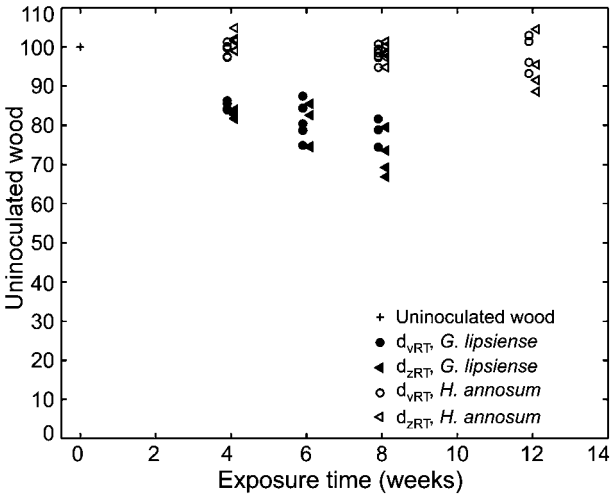

Figure 6 Wave velocity v_{RT} and impedance z_{RT} of inoculated specimens as a function of velocity and impedance of the untreated specimens.

studies of laboratory-decayed wood confirms that the wave velocity and impedance are influenced in the early stages of *H. annosum* decay in Norway spruce by changes in MC rather than by degradation. Since the fungal influence on the MC in laboratory-decayed specimens cannot be conferred to naturally decayed wood, we propose to study the influence of fungi on the MC in standing trees.

Acknowledgements

The inoculation of fungal pathogens by Markus Heeb from EMPA, St. Gallen is gratefully acknowledged.

References

Axmon, J., Hansson, M., Sornmo, L. (2002) Modal analysis of living spruce using a combined Prony and DFT multichannel method for detection of internal decay. Mech. Syst. Signal Proc. 16:561–584.

Axmon, J., Hansson, M., Sornmo, L. (2004) Experimental study on the possibility of detecting internal decay in standing *Picea abies* by blind impact response analysis. Forestry 77:179–192.

Bauer, C., Kilbertus, G. (1991) Ultrasonic technique for determining the extent of fungus attack of beech and pine wood. Holzforschung 45:41–46.

Blanchette, R.A. (1984) Screening wood decayed by white rot fungi for preferential lignin degradation. Appl. Environ. Mircrobiol. 48:647–653.

Blanchette, R.A., Otjen, L., Effland, M.J., Eslyn, W.E. (1985) Changes in structural and chemical components of wood delignified by fungi. Wood Sci. Technol. 19:35–46.

Bucur, V. (1987) Varieties of resonance wood and their elastic constants. J. Catgut Acoust. Soc. 47:42–48.

Bucur, V., Archer, R.R. (1984) Elastic constants for wood by an ultrasonic method. Wood Sci. Technol. 18:255–265.

Demarest, H.H. (1971) Cube-resonance method to determine the elastic constants of solids. J. Acoust. Soc. Am. 49:768–775.

Divos, F., Szalai, L. (2002). Tree evaluation by acoustic tomography, In: 13th International Symposium on Nondestructive Testing of Wood, Berkeley, CA, USA. pp. 251–256.

Dual, J., Hägeli, M., Pfaffinger, M.R., Vollmann, J. (1996) Experimental aspects of quantitative nondestructive evaluation using guided waves. Ultrasonics 34:291–295.

Dumail, J.F., Olofsson, K., Salmén, L. (2000) An analysis of rolling shear of spruce wood by the Iosipescu method. Holzforschung 54:420–426.

Etheridge, D.E. (1955) Comparative studies of North American and European cultures of the root rot fungus, *Fomes annosus* (Fr.). Can. J. Bot. 33:416–428.

Görlacher, R. (2002) A method for determining the rolling shear modulus of timber. Holz Roh- Werkstoff 60:317–322.

Hearmon, R.F.S. The Elasticity of Wood and Plywood. Department of Scientific and Industrial Research, London, 1948.

Hua, Y., Sarkar, T.K. (1990) Matrix pencil method for estimating parameters of exponentially damped undamped sinusoids in noise. IEEE Trans. Acoust. Speech Signal Process. 38:814–824.

Migliori, A., Darling, T., Baiardo, J., Freibert, F. (2001) Resonant ultrasound spectroscopy (RUS). In: Modern Acoustical Techniques for the Measurement of Mechanical Properties, Vol. 39. Ed. Levy, M. Academic Press, San Diego. pp. 189–220.

Neuhaus, H. (1983) Elastic behavior of spruce wood as a function of moisture content. Holz Roh-Werkstoff 41:21–25.

Niemz, P., Graf, E., Lanz, B., Hebeisen, S. (2000) Einfluss des Befalls holzzerstörender Pilze auf Schallgeschwindigkeit und Eigenfrequenz bei Fichten- und Buchenholz. Holzforschung Holzverwertung 6:121–124.

Rayner, A.D.M., Boddy, L. Fungal Decomposition of Wood. Wiley, Chichester, 1988.

Rust, S. (2000). A new tomographic device for the nondestructive testing of trees, In: 12th International Symposium on Nondestructive Testing of Wood, Sopron, Hungary. pp. 233–237.

Schwarze, F.W.M.R. Entwicklung und biomechanische Auswirkungen von holzzersetzenden Pilzen in lebenden Bäumen und in vitro. SVK-Verlag, 1995.

Schwarze, F.W.M.R., Fink, S. (1994) Ermittlung der Holzzersetzung am lebenden Baum. Neue Landschaft 3:182–193.

Schwarze, F.W.M.R., Lonsdale, D., Fink, S. (1997) An overview of wood degradation patterns and their implications for tree hazard assessment. Arboricult. J. 21:1–32.

Stamer, J. (1935) Elastizitätsuntersuchungen an Hölzern. Ing. Arch. 4:1–8.

Wilcox, W.W. (1988) Detection of early stages of wood decay with ultrasonic pulse velocity. For. Prod. J. 38:68–73.

Worrall, J.J., Parmeter, J.R.,Cobb, F.W. (1983) Host specialization of *Heterobasidion annosum*. Phytopathology 73:304–307.

Received May 11, 2005. Accepted September 5, 2005.